

---

# Linear-Time Gromov Wasserstein Distances using Low Rank Couplings and Costs

---

Anonymous Author(s)

Affiliation

Address

email

## Abstract

1 The ability to compare and align related datasets living in heterogeneous spaces  
2 plays an increasingly important role in machine learning. The Gromov-Wasserstein  
3 (GW) formalism can help tackle this problem. Its main goal is to seek an assign-  
4 ment (more generally a coupling matrix) that can register points across otherwise  
5 incomparable datasets. As a non-convex and quadratic generalization of optimal  
6 transport (OT), GW is NP-hard. Yet, heuristics are known to work reasonably  
7 well in practice, the state of the art approach being to solve a sequence of nested  
8 regularized OT problems. While popular, that heuristic remains too costly to scale,  
9 with cubic complexity in the number of samples  $n$ . We show in this paper how a  
10 recent variant of the Sinkhorn algorithm can substantially speed up the resolution of  
11 GW. That variant restricts the set of admissible couplings to those admitting a low  
12 rank factorization as the product of two sub-couplings. By updating alternatively  
13 each sub-coupling, our algorithm computes a stationary point of the problem in  
14 quadratic time with respect to the number of samples. When cost matrices have  
15 themselves low rank, our algorithm has time complexity  $\mathcal{O}(n)$ . We demonstrate  
16 the efficiency of our method on simulated and real data.

## 17 1 Introduction

18 **The ever increasing interest for Gromov-Wasserstein...** Several problems in machine learning  
19 involve comparing families of points that live in heterogeneous spaces. This situation arises typically  
20 when realigning two distinct sets of feature representations obtained from the similar source. Recent  
21 applications to single-cell genomics [15] and NLP [12, 1] provide two cases in point: Thousands  
22 of cells taken from the same tissue are split in two groups, each group is processed with a different  
23 experimental protocol, resulting in two distinct sets of heterogeneous feature vectors; Thousands of  
24 word embeddings for two languages are learned independently. In both cases, one expects to find  
25 a meaningful way to register points across sets living in heterogeneous spaces, since they contain  
26 similar overall information. That realignment is usually carried out using the Gromov-Wasserstein  
27 (GW) machinery proposed by Mémoli [26] and Sturm [36], which seeks a relaxed assignment matrix  
28 that is as “close” to an isometry as possible, using a quadratic score to quantify that closeness. GW  
29 has a lot of practical appeal: It has been used in supervised learning [41], generative modeling [7],  
30 domain adaptation [9], structured prediction [37], quantum chemistry [27] and alignment layers [17].

31 **... despite its cubic cost.** Because it is an NP-hard problem, these applications rely on approximating  
32 GW, typically by solving a sequence of OT problems using entropic regularization. This heuristic is  
33 efficient yet costly, since it requires  $\mathcal{O}(n^3)$  operations to register two sets of  $n$  samples, a price that is  
34 paid when re-instantiating each OT problem. Our goal is to reduce substantially that complexity by  
35 exploiting low-factorization of *both* parameters (data) and variable (relaxed assignment) matrices in  
36 the GW problem, while maintaining state of the art performance in applications.

37 **Wasserstein: from cubic to linear complexity.** A comparatively simpler problem is the registration  
 38 of two populations embedded in the *same* space. This corresponds to the classic optimal transport  
 39 (OT) problem, which has received considerable attention in ML [28]. OT has found applications  
 40 in computer vision [29], NLP [24], single cell tracking [33] or multi-task regression in neuro-  
 41 imaging [22]. While the OT problem is originally cast as a linear program, with a  $O(n^3 \log(n))$  cost,  
 42 many of these works rely on solving instead a penalized OT problem using Sinkhorn’s algorithm [34,  
 43 13]. In its most naive implementation, the Sinkhorn has quadratic complexity [2]. Recent works  
 44 achieve  $O(n)$  complexity by targeting the matrix-vector updates in Sinkhorn’s algorithm using  
 45 low-rank approximations of the data *kernel matrix* [4, 3, 31]. This idea can be further improved by  
 46 imposing the low-rank constraint on the optimization variables of the original OT problem [19], to  
 47 modify Sinkhorn’s steps by enforcing a low rank factorization of the *coupling* variable [32].

48 **Gromov-Wasserstein: from NP-hard to linear approximations.** The GW problem replaces  
 49 the linear objective function in OT by a *non-convex* quadratic objective. Much like OT is a re-  
 50 laxation of the optimal assignment problem, GW can be seen as a relaxation of the quadratic  
 51 assignment problem (QAP). Both GW and QAP are NP-hard to solve [8]. In practice, iteratively  
 52 minimizing a linearization of that quadratic objective using Sinkhorn works surprisingly well [20, 35].  
 53 This method corresponds to a mirror-descent scheme [27],  
 54 and in the special case of Euclidean distance matrices, the loss is concave and it can be also interpreted as a bi-linear  
 55 relaxation [23]. In the most general case, this results in an  $O(n^4)$  algorithm (the objective is a quadratic function of a  
 56  $n \times n$  relaxed assignment matrix), that is reduced to  $O(n^3)$   
 57 when using separable losses [27], a price that remains too  
 58 high for several ML applications. It is possible to replace  
 59 the GW distance by cheaper yet only distantly related proxies,  
 60 such as lower bounds based on OT [26] (see also [30])  
 61 or sliced projections [38]. Whether GW can be efficiently  
 62 sped up remains an open question. We propose in this  
 63 work a novel approach that leverages, as done recently for  
 64 OT, low-rank methods. A very recent line of works attacks  
 65 this problem by quantizing first the two input spaces to  
 66 solve a GW problem of reduced size, thus effectively pro-  
 67 ducing an ad-hoc low-rank coupling [11]. A nice feature  
 68 of this approach is that it maintains the triangular inequality  
 69 and provides a valid upper-bound on the GW distance.  
 70 Related approaches which also approximate GW distance  
 71 using clustering methods (possibly in a recursive way)  
 72 are [6] and [40]. We take in this paper a direct approach:  
 73 instead of separating clustering and GW resolution in 2  
 74 independent steps, we propose do address them simulta-  
 75 neously: our method seeks the least-costly (in GW sense)  
 76 coupling with a low rank constraint, as illustrated in Fig. 1.

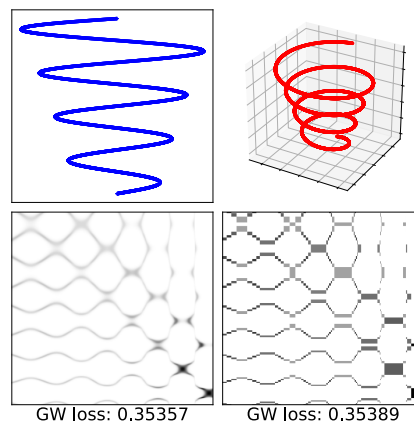


Figure 1: *Top row:* we compute the GW coupling between two curves in 2D and 3D, with  $n = m = 10000$  points. These points are endowed with the squared L2 distance. *Bottom row:* coupling obtained with the SoTA entropic approach [20, 27], compared with our linear method with rank  $r = 10$ . See Appendix D.1 for more details.

79 **Contributions** We introduce the low-rank-GW problem, by imposing a low rank constraint on  
 80 feasible couplings. This method works hand-in-hand with entropic regularization and leads to a  
 81 Sinkhorn-like algorithm. Because of its exclusive reliance on matrix-vector products, the method  
 82 streams well on GPUs. This method can also leverage low-rank factorizations of the input data  
 83 matrices to further reduce the complexity of each iteration to reach linear time. Numerical evaluations  
 84 on simulated and real datasets show that this low-rank approximation maintains the favorable  
 85 property of entropic-regularized GW (namely its ability to compute “good” local minima) for a linear  
 86 computational price, thus paving the way for larger scale uses of GW in ML.

## 87 2 Background on the Gromov-Wasserstein Framework

88 **Comparing measured metric spaces.** Let  $(\mathcal{X}, d_{\mathcal{X}})$  and  $(\mathcal{Y}, d_{\mathcal{Y}})$  be two metric spaces, and  $\mu$  and  
 89  $\nu$  two discrete probability measures on  $\mathcal{X}$  and  $\mathcal{Y}$ , respectively. We write  $\mu := \sum_{i=1}^n a_i \delta_{x_i}$  and  
 90  $\nu := \sum_{j=1}^m b_j \delta_{y_j}$  where  $n, m \geq 1$ ,  $a, b$  are two histograms in the probability simplices  $\Delta_n, \Delta_m$  of  
 91 respective size  $n$  and  $m$ , and  $(x_1, \dots, x_n), (y_1, \dots, y_m)$  are two families in  $\mathcal{X}$  and  $\mathcal{Y}$ . For  $q \geq 1$ ,

92 let us also denote  $A := (d_{\mathcal{X}}^q(x_i, x_{i'}))_{1 \leq i, i' \leq n} \in \mathbb{R}^{n \times n}$  and  $B := (d_{\mathcal{Y}}^q(x_j, x_{j'}))_{1 \leq j, j' \leq m} \in \mathbb{R}^{m \times m}$   
 93 two pairwise cost matrices between the points in the respective supports of  $\mu$  and  $\nu$ . The Gromov-  
 94 Wasserstein (GW) discrepancy between two discrete metric measure spaces  $(\mu, d_{\mathcal{X}})$  and  $(\nu, d_{\mathcal{Y}})$  is  
 95 the solution of the following non-convex quadratic problem, instantiated here for simplicity as a  
 96 function of  $(a, A)$  and  $(b, B)$ , which contain all the information that is needed:

$$\text{GW}((a, A), (b, B)) = \min_{P \in \Pi_{a,b}} \mathcal{E}_{A,B}(P), \text{ where } \Pi_{a,b} := \{P \in \mathbb{R}_+^{n \times m} \mid P\mathbf{1}_m = a, P^T\mathbf{1}_n = b\}, \quad (1)$$

97 and the energy  $\mathcal{E}_{A,B}$  is a quadratic function parameterized by a loss  $L : \mathbb{R} \times \mathbb{R} \rightarrow \mathbb{R}$ :

$$\mathcal{E}_{A,B}(P) := \sum_{i,j,i',j'} L(A_{i,i'}, B_{j,j'}) P_{i,j} P_{i',j'}. \quad (2)$$

98 A typical choice of the loss is the  $L^p$  distance  $L(a, b) = |a - b|^p$  with  $p \geq 1$ . In that case, [26]  
 99 proves that  $\text{GW}^{1/p}$  defines a distance on the space of metric measure spaces quotiented by measure-  
 100 preserving isometries. When  $p = 2$ , as we consider from now on, the GW objective can be evaluated  
 101 efficiently using the marginal constraints imposed on  $P$ , as follows [27]:

$$\mathcal{E}_{A,B}(P) = \langle A^{\odot 2} a, a \rangle + \langle B^{\odot 2} b, b \rangle - 2 \langle APB, P \rangle. \quad (3)$$

102 Indeed, (3) can be computed efficiently in  $\mathcal{O}(n^2 m + nm^2)$  operations, using only matrix/matrix  
 103 multiplications, instead of the  $\mathcal{O}(n^2 m^2)$  complexity of the naive evaluation of (2).

104 **Entropic Gromov-Wasserstein.** The original GW problem (1) can be regularized using an entropic  
 105 term [20, 35, 27], leading to the following problem:

$$\text{GW}_{\varepsilon}((a, A), (b, B)) = \min_{P \in \Pi_{a,b}} \mathcal{E}_{A,B}(P) - \varepsilon H(P), \quad (4)$$

106 where  $H(P) := -\sum_{i,j} P_{i,j} (\log(P_{i,j}) - 1)$  is the entropy of  $P$ . By applying a Mirror  
 107 Descent (MD) scheme with respect to the KL divergence and by choosing the step-size to  
 108 be  $\gamma = 1/\varepsilon$ , Peyré et al. [27] provide a simple algorithm which consists in solving a se-  
 109 quence of regularized OT problem as presented in Algorithm 1. Indeed, each KL  
 110 projection in Algorithm 1 can be computed efficiently thanks to the Sinkhorn algorithm [13].  
 111

112 **Computational complexity.** Given a cost matrix  $C$ , the  
 113 KL projection of  $K_{\varepsilon}$  onto the polytope  $\Pi(a, b)$ , where  
 114  $\text{KL}(P, Q) = \langle P, \log(P/Q) - 1 \rangle$ , is carried out in the inner  
 115 loop of Algo. 1 using the Sinkhorn algorithm, through  
 116 matrix-vector products. This quadratic complexity (in  
 117 red) is dominated by the cost of updating matrix  $C$  at each  
 118 iteration in Algorithm 1, which requires  $\mathcal{O}(n^2 m + nm^2)$   
 119 algebraic operations (cubic, in violet). As noted above,  
 120 evaluating the objective  $\mathcal{E}_{A,B}(P)$  has the same order. In  
 121 the following we show that by considering a low rank  
 122 exact decomposition (or approximation) of the distance  
 123 matrices, the cubic cost of reupdating  $C$  and subsequently  
 124 evaluating  $\mathcal{E}_{A,B}$  can be brought down to quadratic.

---

#### Algorithm 1 Entropic-GW

---

**Inputs:**  $A, B, a, b, \varepsilon$   
 $P = ab^T$  nm  
**for**  $\ell = 0, \dots$  **do**  
 $C \leftarrow -4APB$  nm(n+m)  
 $K_{\varepsilon} \leftarrow \exp(-C/\varepsilon)$  nm  
 $P \leftarrow \underset{P \in \Pi(a,b)}{\text{argmin}} \text{KL}(P, K_{\varepsilon})$   $\mathcal{O}(nm)$   
**end**  
**Result:**  $\mathcal{E}_{A,B}(P)$  nm(n+m)

---

### 125 3 Exploiting a Low-Rank Factorization for Cost Matrices

126 **Exact factorization of cost matrices.** In this section we consider the case where the cost matrices  
 127  $A$  and  $B$  admit a low-rank factorization. More precisely, we make the following assumption.

128 **Assumption 1.** Assume that  $A$  and  $B$  admit a low-rank factorization, that is there exists  $A_1, A_2 \in$   
 129  $\mathbb{R}^{n \times d}$  and  $B_1, B_2 \in \mathbb{R}^{m \times d'}$  such that  $A = A_1 A_2^T$  and  $B = B_1 B_2^T$ , where  $d \ll n, d' \ll m$ .

130 A case in point is when both  $A$  and  $B$  are squared Euclidean distance matrices, with a sample size  
 131 that is larger than ambient dimension. This case is highly relevant, covering many applications of OT  
 132 to ML. The  $d \ll n$  assumption is also likely to hold for most applications, since cases where  $d \gg n$   
 133 are known to pose challenges to the estimation of OT [16, 39]. Writing  $X = [x_1, \dots, x_n] \in \mathbb{R}^{d \times n}$ , if

134  $A = [\|x_i - x_j\|_2^2]_{i,j}$ , then one has, writing  $z = (X^{\odot 2})^T \mathbf{1}_d \in \mathbb{R}^n$  that  $A = z\mathbf{1}_n^T + \mathbf{1}_n z^T - 2X^T X$ .  
 135 Therefore by denoting  $A_1 = [z, \mathbf{1}_n, -\sqrt{2}X^T] \in \mathbb{R}^{n \times (d+2)}$  and  $A_2 = [\mathbf{1}_n, z, \sqrt{2}X^T] \in \mathbb{R}^{n \times (d+2)}$   
 136 we obtain the factorization above.

137 Under Assumption 1, the complexity of Algo. 1 is downgraded to quadratic in sample size: the two  
 138 operations that make Algo. 1 cubic lie in the updates of the cost and the computation of the objective.  
 139 Observe that for any given  $P \in \mathbb{R}^{n \times m}$ , one can compute at each iteration

$$C = -4A_1 A_2^T P B_1 B_2^T$$

140 in  $nm(d + d') + dd'(n + m)$  algebraic operations. Moreover thanks to the reformulation of  
 141  $\mathcal{E}_{A,B}(P)$  given in (3), one can compute it in quadratic time as well. Indeed writing  $G_1 :=$   
 142  $A_1^T P B_2$  and  $G_2 := A_2^T P B_1$ , both in  $\mathbb{R}^{d \times d'}$ , one has  $\langle APB, P \rangle = \mathbf{1}_d^T (G_1 \odot G_2) \mathbf{1}_{d'}$ . Com-  
 143 puting  $G_1, G_2$  given  $P$  requires only  $2(nmd + mdd')$ , and computing their dot product adds  
 144  $dd'$  algebraic operations. The overall complexity to compute  $\mathcal{E}_{A,B}(P)$  is  $\mathcal{O}(nmd + mdd')$ .  
 145

146 **General distance matrices.** When the original  
 147 cost matrices  $A$ , are not low-rank but describe  
 148 distances, we propose to use a recent body of  
 149 work that output their low-rank approximation  
 150 in linear time [5, 21]. These algorithms produce,  
 151 for any distance matrix  $D \in \mathbb{R}^{n \times m}$  and  $\gamma > 0$ ,  
 152 matrices  $D_1 \in \mathbb{R}^{n \times d}$ ,  $D_2 \in \mathbb{R}^{m \times d}$  in  $\mathcal{O}((m +$   
 153  $n)\text{poly}(\frac{d}{\gamma}))$  algebraic operations such that with  
 154 probability at least 0.99 one has

$$\|D - D_1 D_2^T\|_F^2 \leq \|D - C_d\|_F^2 + \gamma \|D\|_F^2$$

155 where  $C_d$  denotes the best rank- $d$  approximation  
 156 to  $D$ . We fall back on this approach to obtain a  
 157 low-rank factorization of a distance matrix in lin-  
 158 ear time whenever needed, aware that this incurs  
 159 an additional approximation. See Appendix B  
 160 for more details.

---

### Algorithm 2 Quadratic Entropic-GW

---

**Inputs:**  $A_1, A_2, B_1, B_2, a, b, \varepsilon$

$P = ab^T$  nm

**for**  $\ell = 0, \dots$  **do**

$G_2 \leftarrow A_2^T P B_1$  nmd + mdd'

$C \leftarrow -4A_1 G_2 B_2^T$  nmd' + ndd'

$K_\varepsilon \leftarrow \exp(-C/\varepsilon)$  nm

$P \leftarrow \underset{P \in \Pi(a,b)}{\text{argmin}} \text{KL}(P, K_\varepsilon)$   $\mathcal{O}(\text{nm})$

**end**

$c_1 \leftarrow \langle A^{\odot 2} a, a \rangle + \langle B^{\odot 2} b, b \rangle$   $\mathcal{O}(\text{nm})$

$G_2 \leftarrow A_2^T P B_1$  nmd + mdd'

$G_1 \leftarrow A_1^T P B_2$  nmd + mdd'

$c_2 \leftarrow -2\mathbf{1}_d^T (G_1 \odot G_2) \mathbf{1}_{d'}$   $\mathcal{O}(\text{dd}')$

$\mathcal{E}_{A,B}(P) \leftarrow c_1 + c_2$

**Return:**  $\mathcal{E}_{A,B}(P)$

---

## 161 4 Imposing a Low Nonnegative Low-Rank for the Coupling

162 In this section, we shift our attention to a different opportunity for speed-ups, *without assuming that*  
 163 *Assumption 1 holds*: we regularize the GW problem by decomposing the coupling as a  
 164 product of two low-rank couplings, in the footsteps of [18, 32], using the following definition:

165 **Definition 1.** Given  $M \in \mathbb{R}^{n \times m}$ , the nonnegative (NN) rank of  $M$  is the smallest number of  
 166 nonnegative rank-one matrices into which the matrix can be decomposed additively:

$$\text{rk}_+(M) := \min \left\{ q \mid M = \sum_{i=1}^q R_i, \forall i, \text{rk}(R_i) = 1, R_i \geq 0 \right\}.$$

167 Following [18, 32], we propose to constrain GW, enforcing a rank  $r$  on the coupling:

$$\text{GW-LR}^{(r)}((a, A), (b, B)) := \min_{P \in \Pi_{a,b}(r)} \mathcal{E}_{A,B}(P), \text{ where } \Pi_{a,b}(r) := \{P \in \Pi_{a,b}, \text{rk}_+(P) \leq r\}. \quad (5)$$

168 Note that the minimum is always attained as  $\Pi_{a,b}(r)$  is compact and the objective is continuous.  
 169 In [32], the authors show that one can parameterize any coupling in  $\Pi_{a,b}(r)$  as a product of two  
 170 low-rank couplings linked by a common marginal. For any  $g \in \Delta_r^*$ , the interior of  $\Delta_r$ , writing

$$\Pi_{a,g,b} := \left\{ P \in \mathbb{R}_+^{n \times m}, P = Q \text{diag}(1/g) R^T, Q \in \Pi_{a,g}, \text{ and } R \in \Pi_{b,g} \right\}.$$

171 one has that  $\bigcup_{g \in \Delta_r^*} \Pi_{a,g,b} = \Pi_{a,b}(r)$ . Therefore GW-LR introduced in (5) can be reformulated as  
 172 the following optimization problem

$$\text{GW-LR}^{(r)}((a, A), (b, B)) = \min_{(Q,R,g) \in \mathcal{C}(a,b,r)} \mathcal{E}_{A,B}(Q \text{diag}(1/g) R^T) \quad (6)$$

173 where  $\mathcal{C}(a, b, r) := \mathcal{C}_1(a, b, r) \cap \mathcal{C}_2(r)$ , with

$$\begin{aligned} \mathcal{C}_1(a, b, r) &:= \left\{ (Q, R, g) \in \mathbb{R}_+^{n \times r} \times \mathbb{R}_+^{m \times r} \times (\mathbb{R}_+^*)^r \text{ s.t. } Q\mathbf{1}_r = a, R\mathbf{1}_r = b \right\}, \\ \mathcal{C}_2(r) &:= \left\{ (Q, R, g) \in \mathbb{R}_+^{n \times r} \times \mathbb{R}_+^{m \times r} \times \mathbb{R}_+^r \text{ s.t. } Q^T\mathbf{1}_n = R^T\mathbf{1}_m = g \right\}. \end{aligned}$$

174 **Stabilization of the Method.** [32] propose to stabilize the objective defined in (6) by adding to the  
 175 constraints a lower bound  $\alpha$  on the weight vector  $g$  such that  $g \geq \alpha$  coordinate-wise. Indeed, as  
 176 a solution of (6) must satisfies  $g > 0$  coordinate-wise, then for  $\alpha$  sufficiently small, the solution  
 177 of the same problem where one adds the constraint  $g \geq \alpha$  will remain the same. Therefore let us  
 178 introduce our new set of constraints  $\mathcal{C}(a, b, r, \alpha) := \mathcal{C}_1(a, b, r, \alpha) \cap \mathcal{C}_2(r)$  where  $\mathcal{C}_1(a, b, r, \alpha) :=$   
 179  $\mathcal{C}_1(a, b, r) \cap \{(Q, R, g) \mid g \geq \alpha\}$ . Another way to stabilize the method is by considering a double  
 180 regularization scheme as proposed in [32] where in addition of constraining the nonnegative rank  
 181 of the coupling, we regularize the objective by adding an entropic term in  $(Q, R, g)$ , which is to be  
 182 understood as that of the values of the three respective entropies evaluated for each term.

$$\text{GW-LR}_{\varepsilon, \alpha}^{(r)}((a, A), (b, B)) := \min_{(Q, R, g) \in \mathcal{C}(a, b, r, \alpha)} \mathcal{E}_{A, B}(Q \text{diag}(1/g)R^T) - \varepsilon H((Q, R, g)). \quad (7)$$

183 **Mirror Descent Scheme.** As in [27], we propose to use a MD scheme with respect to the KL  
 184 divergence to approximate  $\text{GW-LR}_{\varepsilon, \alpha}^{(r)}$  in (7). More precisely, for any  $\varepsilon \geq 0$ , the MD scheme leads  
 185 for all  $k \geq 0$  to the following updates which require solving a convex barycenter problem per step:

$$(Q_{k+1}, R_{k+1}, g_{k+1}) := \underset{\zeta \in \mathcal{C}(a, b, r, \alpha)}{\text{argmin}} \text{KL}(\zeta, \mathbf{K}_k) \quad (8)$$

186 where  $(Q_0, R_0, g_0) \in \mathcal{C}(a, b, r)$  is an initial point such that  $Q_0 > 0$  and  $R_0 > 0$ ,  
 187  $P_k := Q_k \text{diag}(1/g_k)R_k^T$ ,  $\mathbf{K}_k := (K_k^{(1)}, K_k^{(2)}, K_k^{(3)})$ ,  $K_k^{(1)} := \exp(4\gamma AP_k BR_k \text{diag}(1/g_k) -$   
 188  $(\gamma\varepsilon - 1) \log(Q_k))$ ,  $K_k^{(2)} := \exp(4\gamma BP_k^T DQ_k \text{diag}(1/g_k) - (\gamma\varepsilon - 1) \log(R_k))$ ,  $K_k^{(3)} :=$   
 189  $\exp(-4\gamma\omega_k/g_k^2 - (\gamma\varepsilon - 1) \log(g_k))$  with  $[\omega_k]_i := [Q_k^T AP_k BR_k]_{i, i}$  for all  $i \in \{1, \dots, r\}$  and  
 190  $\gamma$  is a positive step size. Solving (8) can be done efficiently thanks to the Dykstra's Algorithm as  
 191 showed in [32]. See Appendix C for more details.

192 **Initialization.** To initialize our algorithm, we adapt the First Lower Bound of [26] to our case of  
 193 interest. More precisely, we show the following Proposition. See appendix A for the proof.

194 **Proposition 1.** *Let us denote  $\tilde{x} = A^{\odot 2}a \in \mathbb{R}^n$ ,  $\tilde{y} = B^{\odot 2}b \in \mathbb{R}^m$  and  $\tilde{C} = (|\tilde{x}_i - \tilde{y}_j|^2)_{i, j} \in \mathbb{R}^{n \times m}$ .*  
 195 *Then for all  $\varepsilon \geq 0$  and  $r \geq 1$  we have,*

$$\text{GW-LR}^{(r)}((a, A), (b, B)) \geq \min_{(Q, R, g) \in \mathcal{C}(a, b, r, \alpha)} \langle \tilde{C}, Q \text{diag}(1/g)R^T \rangle - \varepsilon H((Q, R, g)). \quad (9)$$

196 Note that the RHS of the inequality (9) is exactly the problem studied in [32] for which an algorithm  
 197 was proposed. Therefore to initialize our algorithm, we propose to use their approach. Note that here  
 198 the cost  $\tilde{C}$  is the squared Euclidean distance between two families  $\{\tilde{x}_1, \dots, \tilde{x}_n\}$  and  $\{\tilde{y}_1, \dots, \tilde{y}_m\}$   
 199 in 1-D which admits a low-rank factorization. Therefore we can apply the linear-time version of the  
 200 algorithm presented in [32] to compute the solution. Algorithm 3 summarizes our approach, where  
 201  $\mathcal{D}(\cdot)$  denotes the operator extracting the diagonal of a square matrix.

202 **Computational Cost.** Computing the initialization goes through the computations of  $\tilde{x}$  and  $\tilde{y}$  which  
 203 requires  $\mathcal{O}(n^2 + m^2)$  algebraic operations. Moreover, applying the algorithm proposed in [32]  
 204 when the underlying cost is the squared Euclidean distances between two families in 1-D needs  
 205 only  $\mathcal{O}((n + m)r)$  algebraic operations. Solving the barycenter problem as defined in (8) can be  
 206 done efficiently thanks to Dykstra's Algorithm. Indeed in [32, Algorithm 2] the authors show that  
 207 given  $(K_k^{(1)}, K_k^{(2)}, K_k^{(3)})$ , each iteration of their algorithm requires only  $\mathcal{O}((n + m)r)$  algebraic  
 208 operations since it involves only matrix/vector multiplications. However computing the kernel  
 209 matrices  $(K_k^{(1)}, K_k^{(2)}, K_k^{(3)})$  at each iteration of Algorithm 3 requires a quadratic complexity with  
 210 respect to the number of samples. Overall the proposed algorithm, while faster than the cubic  
 211 implementation proposed in [27], still needs  $\mathcal{O}((n^2 + m^2)r)$  operations per iteration. In the following  
 212 we will see that by combining both nonnegative low-rank constraints on the coupling and low-rank  
 213 approximations of the distance matrices, we can obtain a linear time algorithm with respect to the  
 214 number of samples which computes an approximation of the GW distance.

---

**Algorithm 3** Low-Rank GW, GW-LR $_{\varepsilon, \alpha}^{(r)}((a, A), (b, B))$ 


---

**Inputs:**  $A, B, a, b, r, \varepsilon, \alpha$ 
 $\tilde{x} \leftarrow A^{\odot 2} a, \tilde{y} \leftarrow B^{\odot 2} b \quad \mathcal{O}(m^2 + n^2) \quad \leftarrow \text{Step } (\star)$ 
 $z_1 \leftarrow \tilde{x}^{\odot 2}, z_2 \leftarrow \tilde{y}^{\odot 2} \quad \mathcal{O}(m + n)$ 
 $\tilde{C}_1 \leftarrow [z_1, \mathbf{1}_n, -\sqrt{2}\tilde{x}], \tilde{C}_2 \leftarrow [\mathbf{1}_m, z_2, \sqrt{2}\tilde{y}]^T \quad \mathcal{O}(n + m)$ 
 $(Q, R, g) \leftarrow \underset{(Q, R, g) \in \mathcal{C}(a, b, r, \alpha)}{\operatorname{argmin}} \langle \tilde{C}_1 \tilde{C}_2, Q \operatorname{diag}(1/g) R^T \rangle - \varepsilon H((Q, R, g)) \quad \mathcal{O}((n + m)r)$ 
**for**  $k = 1, \dots$  **do**
 $C_1 \leftarrow -AQ \operatorname{diag}(1/g), C_2 \leftarrow R^T B \quad \mathcal{O}((n^2 + m^2)r) \quad \leftarrow \text{Step } (\star\star)$ 
 $K^{(1)} \leftarrow \exp(4\gamma C_1 C_2 R \operatorname{diag}(1/g) - (\gamma\varepsilon - 1) \log(Q)) \quad \mathcal{O}((m + n)r^2)$ 
 $K^{(2)} \leftarrow \exp(4\gamma C_2^T C_1^T Q \operatorname{diag}(1/g) - (\gamma\varepsilon - 1) \log(R)) \quad \mathcal{O}((m + n)r^2)$ 
 $\omega \leftarrow \mathcal{D}(Q^T C_1 C_2 R), K^{(3)} \leftarrow \exp(-4\gamma\omega/g^2 - (\gamma\varepsilon - 1) \log(g)) \quad \mathcal{O}(nr^2)$ 
 $(Q, R, g) \leftarrow \underset{\zeta \in \mathcal{C}(a, b, r, \alpha)}{\operatorname{argmin}} \operatorname{KL}(\zeta, (K^{(1)}, K^{(2)}, K^{(3)})) \quad \mathcal{O}((m + n)r)$ 
**end**
 $c_1 \leftarrow \langle \tilde{x}, a \rangle + \langle \tilde{y}, b \rangle \quad n + m$ 
 $C_1 \leftarrow -AQ \operatorname{diag}(1/g), C_2 \leftarrow R^T B \quad \mathcal{O}((n^2 + m^2)r) \quad \leftarrow \text{Step } (\star\star)$ 
 $G \leftarrow C_2 R, G \leftarrow C_1 G, G \leftarrow Q^T G \operatorname{diag}(1/g) \quad \mathcal{O}((m + n)r^2)$ 
 $c_2 \leftarrow -2\operatorname{Tr}(G) \quad r$ 
 $\mathcal{E} \leftarrow c_1 + c_2$ 
**Return:**  $\mathcal{E}$ 


---

215 **Convergence of the mirror descent.** Even if the objective (7) is not convex in  $(Q, R, g)$ , we obtain  
 216 the non-asymptotic stationary convergence of the MD algorithm in this setting. For that purpose  
 217 we consider the same convergence criterion as the one proposed in [32] to obtain non-asymptotic  
 218 stationary convergence of the MD scheme defined as

$$\Delta_{\varepsilon, \alpha}(\xi, \gamma) := \frac{1}{\gamma^2} (\operatorname{KL}(\xi, \mathcal{G}_{\varepsilon, \alpha}(\xi, \gamma)) + \operatorname{KL}(\mathcal{G}_{\varepsilon, \alpha}(\xi, \gamma), \xi))$$

219 where  $\mathcal{G}_{\varepsilon, \alpha}(\xi, \gamma) := \underset{\zeta \in \mathcal{C}(a, b, r, \alpha)}{\operatorname{argmin}} \{ \langle \nabla \mathcal{E}_{A, B}(\xi), \zeta \rangle + \frac{1}{\gamma} \operatorname{KL}(\zeta, \xi) \}$ . For any  $1/r \geq \alpha > 0$ , we  
 220 show in the following proposition the non-asymptotic stationary convergence of the MD scheme  
 221 applied to the problem (7). See Appendix A for the proof.

222 **Proposition 2.** Let  $\varepsilon \geq 0$ ,  $\frac{1}{r} \geq \alpha > 0$  and  $N \geq 1$ . By denoting  $L_{\varepsilon, \alpha} := 27(\|A\|_2 \|B\|_2 / \alpha^4 + \varepsilon)$   
 223 and by considering a constant stepsize in the MD scheme (8)  $\gamma = \frac{1}{2L_{\varepsilon, \alpha}}$ , we obtain that

$$\min_{1 \leq k \leq N} \Delta_{\varepsilon, \alpha}((Q_k, R_k, g_k), \gamma) \leq \frac{4L_{\varepsilon, \alpha} D_0}{N}.$$

224 where  $D_0 := \mathcal{E}_{A, B}(Q_0 \operatorname{diag}(1/g_0) R_0^T) - \text{GW-LR}^{(r)}((a, A), (b, B))$  is the distance of the initial value  
 225 to the optimal one.

226 Recall that for  $\alpha$  sufficiently small, we have  $\text{GW-LR}_{\varepsilon, \alpha}^{(r)}((a, A), (b, B)) = \text{GW-LR}_{\varepsilon}^{(r)}((a, A), (b, B))$ .  
 227 Thus Proposition 2 show that our algorithm reach a stationary point of (7). In particular, if  $\varepsilon = 0$ , the  
 228 proposed algorithm converges towards a stationary point of (5).

## 229 5 Double Low-rank Approach for Linear Time GW

230 Almost all operations in Algorithm 3 are linear time, except for the three updates highlighted in  
 231 red, involving  $C_1$  and  $C_2$ , and the computations of  $\tilde{x} = A^{\odot 2} a$  and  $\tilde{y} = B^{\odot 2} b$  as they still require a  
 232 quadratic number of algebraic operations. When adding Assumption 1 from §3 to the rank constrained  
 233 approach from §4, we notice that the strengths of both approaches can work hand in hand, both in  
 234 easier initial evaluations of  $\tilde{x}, \tilde{y}$ , but, most importantly, at each new recomputation of a *factorized*  
 235 linearization of the quadratic objective:

**Linear time outer norms.** Because  $A$  admits a low-rank factorization, one can obtain a low-rank  
 factorization for  $A^{\odot 2}$ . Indeed, remark that for  $x, y \in \mathbb{R}^d$ ,  $\langle x, y \rangle^2 = \sum_{i, j=1}^d x_i x_j y_i y_j$ . Therefore

by studying the rows of matrices  $A_1 := [a_1^{(1)}; \dots; a_n^{(1)}]$  and  $A_2 := [a_1^{(2)}; \dots; a_n^{(2)}]$ , if one writes  $\psi(x) := \text{Vect}(xx^T) \in \mathbb{R}^{d^2}$  where  $\text{Vect}(\cdot)$  is the vectorization operation, we obtain that

$$A^{\odot 2} = \tilde{A}_1 \tilde{A}_2^T \text{ where } \tilde{A}_1 = [\psi(a_1^{(1)}), \dots, \psi(a_n^{(1)})]^T, \tilde{A}_2 = [\psi(a_1^{(2)}), \dots, \psi(a_n^{(2)})]^T.$$

236 In Algorithm 3, the line “Step  $(\star)$ ” can thus be replaced by  $\tilde{x} \leftarrow \tilde{A}_1 \tilde{A}_2^T a$  and  $\tilde{y} \leftarrow \tilde{B}_1 \tilde{B}_2^T b$ . Note  
 237 that computing  $\tilde{A}_1$  given  $A_1$  requires only  $\mathcal{O}(nd^2)$  operations, so that this alternate code only takes  
 238  $\mathcal{O}(nd^2) + \mathcal{O}(m(d')^2)$  operations.

239 **Linear time linearization of the GW objective.** The linearization step, the critical step in Algo.1  
 240 that consists in updating  $C$  at each iteration, consumes a substantial portion of the computational  
 241 budget of GW. Introducing the low-rank Sinkhorn approach makes this step quadratic in Algo.3; the  
 242 complexity of that step is also quadratic using the low-rank assumption on costs  $A$  and  $B$ , in Algo.2.  
 243 There is therefore an opportunity to marry both to speed-up that important step. We argue that this is  
 244 indeed what happens, in the sense that combining the two yields indeed linear time complexities in  
 245 sample sizes, by replacing in Algorithm 3, the lines “Step  $(\star\star)$ ” by

$$C_1 \leftarrow -A_1 A_2^T Q \text{diag}(1/g) \quad \text{and} \quad C_2 \leftarrow R^T B_2 B_1^T.$$

246 Note that this speed-up would not be achieved using other approaches that output a low rank  
 247 approximation of the transport plan [4, 3, 31]. The crucial obstacle to using these methods here is that  
 248 the cost matrix  $C$  in GW is “synthetic”, in the sense that it is the output of a matrix product  $APB$   
 249 involving the very last transport  $P$ . This stands in stark contrast with the requirements in [4, 3, 31]  
 250 that the *kernel* matrix corresponding to  $K_\varepsilon = e^{-C/\varepsilon}$  admits favorable properties, such as being p.s.d  
 251 or admitting an explicit (random or not) finite dimensional feature approximation. Since  $C$  changes  
 252 at each iteration in Algo.1, they are not directly applicable.

253 Combining the results in §4 with those from §B results in updates for  $C_1$  and  $C_2$  that only require  
 254  $\mathcal{O}(nrd)$  and  $\mathcal{O}(mrd')$  operations.

255 **Linear time GW.** Finally all the quadratic operations appearing in Algorithm (3) can be replaced  
 256 by linear counterparts. The iterations that have not been modified had an overall complexity of  
 257  $\mathcal{O}(mr(r+d) + nr(r+d))$  at each iteration. The initialization and linearization steps can now be  
 258 performed in linear time, with respective complexity of respectively  $\mathcal{O}(n(r+d^2) + m((d')^2 + r))$   
 259 and  $\mathcal{O}((nr(r+d) + mr(r+d')))$ .

## 260 6 Experiments

261 Our goal in this section is to demonstrate that, for a far smaller computational budget, the GW-LR  
 262 approach is competitive with the direct entropic approach on datasets that are either synthesized  
 263 to exhibit local clusters, or directly validated on a real high-dimensional dataset as well. Because  
 264 both approaches have different hyperparameters, our goal is to stick to a realistic evaluation that  
 265 stresses both optimality of solutions as a function of computational effort, as well as performance  
 266 in real life applications. We start by investigating the sensitivity of hyperparameters  $\varepsilon$  and  $\gamma$  on our  
 267 method. Since GW is not convex, these may interact in unexpected ways. Experiments were run on a  
 268 personal MacBook Pro 2019 laptop. We reused code from [github.com/meyerscetton/LOT](https://github.com/meyerscetton/LOT), and  
 269 downloaded genomics data from [github.com/rsinghlab/SCOT](https://github.com/rsinghlab/SCOT).

270 **Benchmarks.** We consider three synthetic problems and one real world problem to evaluate time-  
 271 accuracy trade-offs, and also compare the couplings obtained by our method and that of the entropic  
 272 version [27]. More precisely, we compare the quadratic approach in **GW-LR** computed with  
 273 algorithm (3) (and its linear time counterpart, **Lin GW-LR** as presented in §5), with **Entropic-**  
 274 **GW**, the cubic implementation of [27] (as well as its quadratic counterpart, **Quad Entropic-GW**  
 275 presented in Algo. 2). For **GW-LR** and **Lin GW-LR**, and in all experiments, we set the lower bound  
 276 on entries of  $g$  to  $\alpha = 10^{-10}$ .

277 **Initialization** To initialize all algorithms with a common strategy, we adapted the *first lower bound*  
 278 of [26, Def. 6.1] to the entropic case. In all experiments showing time-accuracy tradeoffs, we choose  
 279 to use number of operations to provide platform independent quantities. Accuracy is measured  
 280 by evaluating the ground-truth energy  $\mathcal{E}_B$  (even in scenarios when the method uses a low rank  
 281 approximation for  $A, B$  at optimization time).

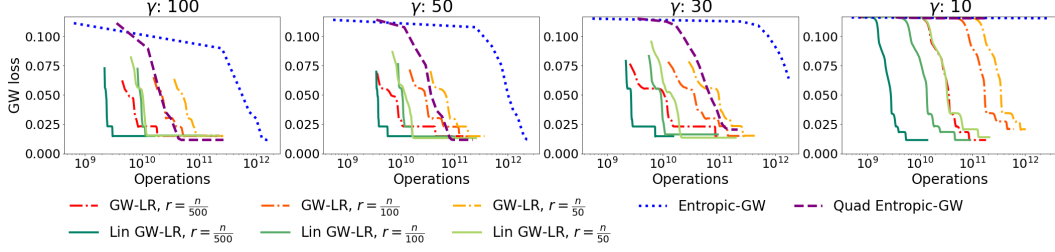


Figure 3: The number of cluster in each distribution is 10 and the number of samples is  $n = m = 5000$ . The ground cost is the Euclidean distance. As we can evaluate the distance between two arbitrary points, we can obtain in linear-time an efficient approximation of the distance matrices  $A$  and  $B$  as presented in 3. The rank of their factorizations is fixed to be  $d = d' = 100$ . **GW-LR** and **Entropic-GW** corresponds to the case where the full matrices  $A$  and  $B$  are considered while **Lin GW-LR** and **Quad Entropic-GW** take as inputs the low-rank approximations of the distance matrices. We plot the time-accuracy tradeoff for multiple choices of  $\gamma$  and rank  $r$  defined as a fraction of  $n$ . For **Entropic-GW** and **Quad Entropic-GW**, we set  $\varepsilon = 1/\gamma$  as proposed in [27]. Recall that for low-rank methods, we set  $\varepsilon = 0$ .

282 **Sensitivity to  $\gamma$  and  $\varepsilon$**  Here we aim at showing the  
 283 dependence in both  $\gamma$  and  $\varepsilon$  of our proposed method.  
 284 In Figure 2, we compare the GW loss obtained by our  
 285 algorithm when varying  $\varepsilon$  and  $\gamma$  on two mixtures. We  
 286 show that when  $\varepsilon = 0$ , the proposed method manage  
 287 to consistently obtain small GW loss whatever  $\gamma$  is.  
 288 By allowing  $\varepsilon > 0$ , the algorithm is able to reach even  
 289 smaller GW loss, however, the choice of  $\varepsilon$  depends  
 290 highly on  $\gamma$ . Therefore in the following experiments,  
 291 we fix  $\varepsilon = 0$  for our method. We also show the  
 292 dependence in  $\gamma$  and  $\varepsilon$  of our method in other settings  
 293 and observe similar behaviors. See Appendix D.2 for  
 294 more details.

295 **Remark 1.** As shown in Figure 8 in Appendix D.2,  
 296 allowing  $\varepsilon > 0$  may also increase the speed of con-  
 297 vergence of the algorithm. However choosing well  $\varepsilon$   
 298 for a given  $\gamma$  must be done carefully and we prefer in  
 299 the following experiments to present the performance  
 300 of our method in the simplest setting where  $\varepsilon = 0$ .

301 **Synthetic low-rank problem** In this experiment  
 302 we aim at comparing the time-accuracy tradeoff of  
 303 the different methods when the underlying distribu-  
 304 tions has a low-rank structure. For that purpose, we  
 305 consider two distributions in respectively 10-D and  
 306 15-D, where the support of each distributions is the  
 307 concatenation of clusters of points, and where the eu-  
 308 clidean distance between the centroids of the clusters  
 309 is bigger than a threshold  $\beta$ . Here we set  $\beta = 10$ .  
 310 Both distributions are uniform, have the same number  
 311 of clusters and the same number of points in each cluster. Some illustrations of the simulated data  
 312 is provided in Appendix D.3. In Figure 3, when the underlying cost is the (not squared) Euclidean  
 313 distance, our methods manage to consistently obtain similar accuracy that the ones obtained by  
 314 entropic methods, with very low rank  $r = n/500$ , while being orders of magnitude faster. In Figure 4,  
 315 we also compare the time-accuracy tradeoffs in the more favorable case where the underlying cost  
 316 is the squared Euclidean distance and obtain similar results. We also show more experiments for  
 317 different number of clusters in Appendix D.3, leading to similar conclusions.

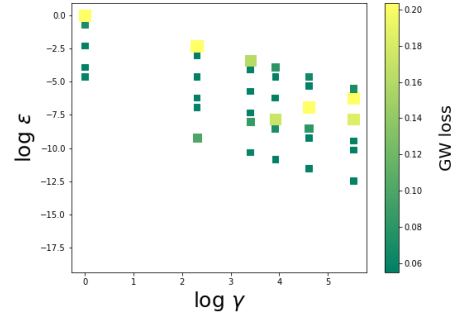


Figure 2: In this experiment, we consider two mixtures of (2 and 3) Gaussians in respectively 5-D and 10-D, sampled as discrete measures with  $n = m = 5000$  points, see more details on setup in Appendix D.2. The ground cost is the squared Euclidean distance, which provides an exact low-rank factorization of the cost as presented in § 3. Results on speed (in Appendix) are therefore obtained using **Lin GW-LR**. The nonnegative rank of the coupling is set to  $r = 50 = n/100$ . We plot the GW loss obtained by **Lin GW-LR** when varying  $\varepsilon$  for multiple choices of  $\gamma$ . Both size and color have been used to quantify visually the value of the loss at that parameter pair. Occasional inversions are due to the nonconvex nature of the GW problem.



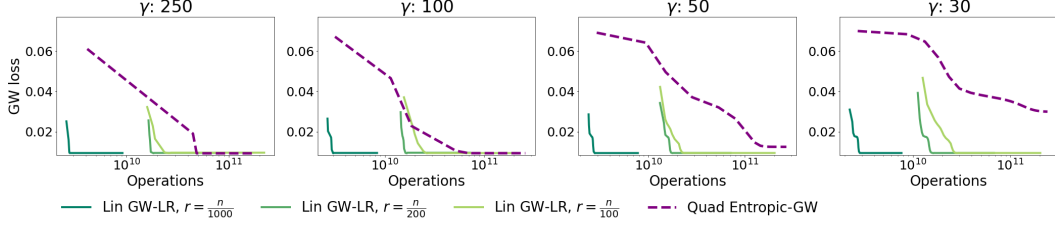


Figure 4: The number of clusters in each distribution is 5 and the number of samples considered here is  $n = m = 10000$ . The ground cost is the squared Euclidean distance. We compare **Lin GW-LR** and **Quad Entropic-GW** as we have an exact factorization of the matrices  $A$  and  $B$ . We plot the time-accuracy tradeoff when varying  $\gamma$  for multiple choices of  $r$ . For **Quad Entropic-GW**, we set  $\varepsilon = 1/\gamma$  and for **Lin GW-LR** we set  $\varepsilon = 0$ .

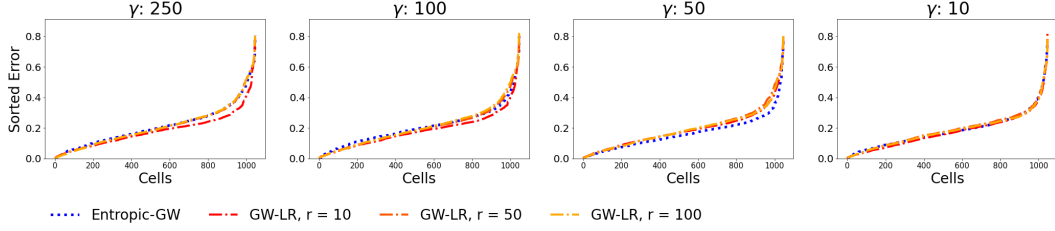


Figure 5: We plot, for each cells of the SNAREseq dataset, the FOSCTTM ranked in the increasing order for both **GW-LR** and **Entropic-GW**.

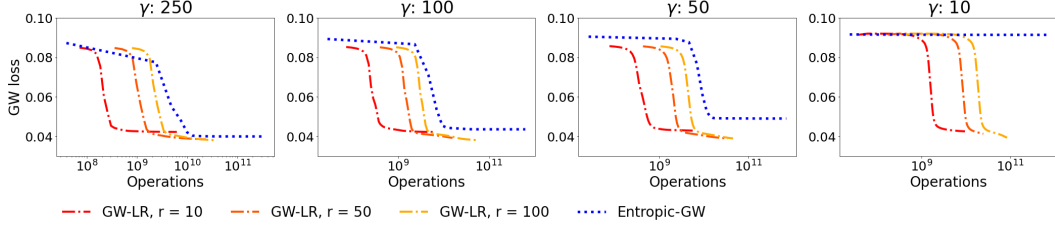


Figure 6: Plot of the time-accuracy tradeoff when varying  $\gamma$  for multiple choices of rank  $r$  on the SNAREseq dataset. For **Entropic-GW** we set  $\varepsilon = 1/\gamma$ , for **GW-LR**, we set  $\varepsilon = 0$ .

318 **Experiments on Single Cell Genomics Data.** We reproduce the single-cell alignment experiment  
 319 introduced in [14]. The dataset consists in single-cell multi-omics data generated by co-assays. In  
 320 that setup, the ground truth one-to-one correspondence information between cells is known, and can  
 321 therefore be used to benchmark GW strategies. The dataset considered is the SNAREseq [10], with  
 322  $n = m = 1047$ . We apply the exact same pre-processing steps as proposed in [14] by computing  
 323 intra-domain distance matrices  $A$  and  $B$  with a k-NN graphs based on correlations, to compute  
 324 shortest path distance matrices. Note that in that case, one cannot obtain directly in linear time a  
 325 low-rank factorization of  $A$  and  $B$  using [5, 21], since the shortest path distances need to be computed  
 326 first. Therefore we only consider the quadratic **GW-LR** and the cubic **Entropic-GW**. In Figure 6,  
 327 we compare the alignment performance through the “fraction of samples closer than the true match”  
 328 (FOSCTTM) introduced in [25]. We see that both algorithm obtain similar performance. However, in  
 329 Figure 5, we show that whatever the  $\gamma$  chosen, **GW-LR** reaches better accuracy while being order of  
 330 magnitude faster than **Entropic-GW** for a very small rank  $r = 10$ .

331 **Conclusion.** While the factorization introduced in [32] held the promise to speed up classic OT, we  
 332 have shown in this work that it delivers an even larger impact when applied to the GW problem:  
 333 Indeed, the combination of low-rank Sinkhorn factorization with low rank cost matrices is the only  
 334 one, to our knowledge, that ensures that the linearization step of the GW objective can be carried out  
 335 with a linear complexity, throughout outer iterations. This linear complexity is comparable to that of  
 336 the most recent OT solvers, yet still retains the appealing properties of the Entropic approach, such as  
 337 stability and convergence to meaningful solutions.

338 **References**

- 339 [1] Jean Alaux, Edouard Grave, Marco Cuturi, and Armand Joulin. Unsupervised hyperalignment  
340 for multilingual word embeddings. *arXiv preprint arXiv:1811.01124*, 2018.
- 341 [2] Jason Altschuler, Jonathan Weed, and Philippe Rigollet. Near-linear time approximation  
342 algorithms for optimal transport via sinkhorn iteration. *arXiv preprint arXiv:1705.09634*, 2017.
- 343 [3] Jason Altschuler, Francis Bach, Alessandro Rudi, and Jonathan Niles-Weed. Massively scalable  
344 sinkhorn distances via the nyström method, 2018.
- 345 [4] Jason Altschuler, Francis Bach, Alessandro Rudi, and Jonathan Weed. Approximating the  
346 quadratic transportation metric in near-linear time. *arXiv preprint arXiv:1810.10046*, 2018.
- 347 [5] Ainesh Bakshi and David P. Woodruff. Sublinear time low-rank approximation of distance  
348 matrices, 2018.
- 349 [6] Andrew J Blumberg, Mathieu Carriere, Michael A Mandell, Raul Rabadan, and Soledad Villar.  
350 Mrec: a fast and versatile framework for aligning and matching point clouds with applications  
351 to single cell molecular data. *arXiv preprint arXiv:2001.01666*, 2020.
- 352 [7] Charlotte Bunne, David Alvarez-Melis, Andreas Krause, and Stefanie Jegelka. Learning  
353 generative models across incomparable spaces. *arXiv preprint arXiv:1905.05461*, 2019.
- 354 [8] Rainer E Burkard, Eranda Cela, Panos M Pardalos, and Leonidas S Pitsoulis. The quadratic  
355 assignment problem. In *Handbook of combinatorial optimization*, pages 1713–1809. Springer,  
356 1998.
- 357 [9] Laetitia Chapel, Mokhtar Alaya, and Gilles Gasso. Partial optimal transport with applications  
358 on positive-unlabeled learning. In *Advances in Neural Information Processing Systems 33*  
359 (*NeurIPS 2020*), 2020.
- 360 [10] Song Chen, Blue B Lake, and Kun Zhang. High-throughput sequencing of the transcriptome  
361 and chromatin accessibility in the same cell. *Nature biotechnology*, 37(12):1452–1457, 2019.
- 362 [11] Samir Chowdhury, David Miller, and Tom Needham. Quantized gromov-wasserstein. *arXiv*  
363 *preprint arXiv:2104.02013*, 2021.
- 364 [12] Alexis Conneau, Guillaume Lample, Marc’Aurelio Ranzato, Ludovic Denoyer, and Hervé  
365 Jégou. Word translation without parallel data. *arXiv preprint arXiv:1710.04087*, 2017.
- 366 [13] Marco Cuturi. Sinkhorn distances: Lightspeed computation of optimal transport. In *Advances*  
367 *in neural information processing systems*, pages 2292–2300, 2013.
- 368 [14] Pinar Demetci, Rebecca Santorella, Björn Sandstede, William Stafford Noble, and Ritambhara  
369 Singh. Gromov-wasserstein optimal transport to align single-cell multi-omics data. *bioRxiv*,  
370 2020. doi: 10.1101/2020.04.28.066787.
- 371 [15] Pinar Demetci, Rebecca Santorella, Bjorn Sandstede, William Stafford Noble, and Ritambhara  
372 Singh. Gromov-wasserstein optimal transport to align single-cell multi-omics data. *BioRxiv*,  
373 2020.
- 374 [16] Richard Mansfield Dudley et al. Weak convergence of probabilities on nonseparable metric  
375 spaces and empirical measures on euclidean spaces. *Illinois Journal of Mathematics*, 10(1):  
376 109–126, 1966.
- 377 [17] Danielle Ezuz, Justin Solomon, Vladimir G Kim, and Mirela Ben-Chen. Gwcn: A metric  
378 alignment layer for deep shape analysis. In *Computer Graphics Forum*, volume 36, pages 49–57.  
379 Wiley Online Library, 2017.
- 380 [18] Aden Forrow, Jan-Christian Hütter, Mor Nitzan, Philippe Rigollet, Geoffrey Schiebinger, and  
381 Jonathan Weed. Statistical optimal transport via factored couplings, 2018.
- 382 [19] Aden Forrow, Jan-Christian Hütter, Mor Nitzan, Philippe Rigollet, Geoffrey Schiebinger, and  
383 Jonathan Weed. Statistical optimal transport via factored couplings. In *The 22nd International*  
384 *Conference on Artificial Intelligence and Statistics*, pages 2454–2465. PMLR, 2019.
- 385 [20] Steven Gold and Anand Rangarajan. Softassign versus softmax: Benchmarks in combinatorial  
386 optimization. *Advances in neural information processing systems*, pages 626–632, 1996.
- 387 [21] Piotr Indyk, Ali Vakilian, Tal Wagner, and David Woodruff. Sample-optimal low-rank approxi-  
388 mation of distance matrices, 2019.

- 389 [22] Hicham Janati, Thomas Bazeille, Bertrand Thirion, Marco Cuturi, and Alexandre Gramfort.  
390 Multi-subject meg/eeg source imaging with sparse multi-task regression. *NeuroImage*, page  
391 116847, 2020.
- 392 [23] Hiroshi Konno. Maximization of a convex quadratic function under linear constraints. *Mathe-*  
393 *matical programming*, 11(1):117–127, 1976.
- 394 [24] Matt Kusner, Yu Sun, Nicholas Kolkin, and Kilian Q Weinberger. From word embeddings to  
395 document distances. In *Proc. of the 32nd Intern. Conf. on Machine Learning*, pages 957–966,  
396 2015.
- 397 [25] Jie Liu, Yuanhao Huang, Ritambhara Singh, Jean-Philippe Vert, and William Stafford Noble.  
398 Jointly embedding multiple single-cell omics measurements. *BioRxiv*, page 644310, 2019.
- 399 [26] Facundo Mémoli. Gromov–wasserstein distances and the metric approach to object matching.  
400 *Foundations of computational mathematics*, 11(4):417–487, 2011.
- 401 [27] Gabriel Peyré, Marco Cuturi, and Justin Solomon. Gromov-wasserstein averaging of kernel and  
402 distance matrices. In *International Conference on Machine Learning*, pages 2664–2672, 2016.
- 403 [28] Gabriel Peyré and Marco Cuturi. Computational optimal transport. *Foundations and Trends in*  
404 *Machine Learning*, 11(5-6), 2019. ISSN 1935-8245.
- 405 [29] Yossi Rubner, Carlo Tomasi, and Leonidas J. Guibas. The earth mover’s distance as a metric for  
406 image retrieval. *International Journal of Computer Vision*, 40(2):99–121, November 2000.
- 407 [30] Ryoma Sato, Marco Cuturi, Makoto Yamada, and Hisashi Kashima. Fast and robust comparison  
408 of probability measures in heterogeneous spaces. *arXiv preprint arXiv:2002.01615*, 2020.
- 409 [31] Meyer Scetbon and Marco Cuturi. Linear time sinkhorn divergences using positive features,  
410 2020.
- 411 [32] Meyer Scetbon, Marco Cuturi, and Gabriel Peyré. Low-rank sinkhorn factorization, 2021.
- 412 [33] Geoffrey Schiebinger, Jian Shu, Marcin Tabaka, Brian Cleary, Vidya Subramanian, Aryeh  
413 Solomon, Joshua Gould, Siyan Liu, Stacie Lin, Peter Berube, et al. Optimal-transport analysis  
414 of single-cell gene expression identifies developmental trajectories in reprogramming. *Cell*, 176  
415 (4):928–943, 2019.
- 416 [34] Richard Sinkhorn. A relationship between arbitrary positive matrices and doubly stochastic  
417 matrices. *Ann. Math. Statist.*, 35:876–879, 1964.
- 418 [35] Justin Solomon, Gabriel Peyré, Vladimir G Kim, and Suvrit Sra. Entropic metric alignment for  
419 correspondence problems. *ACM Transactions on Graphics (TOG)*, 35(4):1–13, 2016.
- 420 [36] Karl-Theodor Sturm. The space of spaces: curvature bounds and gradient flows on the space of  
421 metric measure spaces. *arXiv preprint arXiv:1208.0434*, 2012.
- 422 [37] Titouan Vayer, Laetitia Chapel, Rémi Flamary, Romain Tavenard, and Nicolas Courty. Fused  
423 gromov-wasserstein distance for structured objects: theoretical foundations and mathematical  
424 properties. *arXiv preprint arXiv:1811.02834*, 2018.
- 425 [38] Titouan Vayer, Rémi Flamary, Romain Tavenard, Laetitia Chapel, and Nicolas Courty. Sliced  
426 gromov-wasserstein. *arXiv preprint arXiv:1905.10124*, 2019.
- 427 [39] Jonathan Weed and Francis Bach. Sharp asymptotic and finite-sample rates of convergence of  
428 empirical measures in wasserstein distance. *Bernoulli*, 25(4A):2620–2648, 2019.
- 429 [40] Hongteng Xu, Dixin Luo, and Lawrence Carin. Scalable gromov-wasserstein learning for graph  
430 partitioning and matching. *arXiv preprint arXiv:1905.07645*, 2019.
- 431 [41] Hongteng Xu, Dixin Luo, Hongyuan Zha, and Lawrence Carin Duke. Gromov-wasserstein  
432 learning for graph matching and node embedding. In *International conference on machine*  
433 *learning*, pages 6932–6941. PMLR, 2019.

## 434 Checklist

- 435 1. For all authors...

- 436 (a) Do the main claims made in the abstract and introduction accurately reflect the paper’s  
437 contributions and scope? [Yes] The main claim of the paper is a linear time (w.r.t.  
438 sample size, as commonly understood in OT) computation for GW. Sections §3,4 and 5  
439 build up that answer. This is experimentally validated across several experiments, both  
440 synthetic, to help the reader form intuitions, and on real data where GW was deemed  
441 useful.
- 442 (b) Did you describe the limitations of your work?[Yes] Because the GW problem is non-  
443 convex, these limitations are naturally discussed in the experimental section, Section §6.  
444 We discuss the effects of  $\gamma$  and  $\varepsilon$  on the method, which are not easy to parse due to the  
445 non-convexity of the method.
- 446 (c) Did you discuss any potential negative societal impacts of your work?[N/A] As a purely  
447 methodological paper, we do not envision potentially negative impact of this work on  
448 its own.
- 449 (d) Have you read the ethics review guidelines and ensured that your paper conforms to  
450 them?[Yes] We have read these guidelines and confirm our paper does conform to  
451 them.
- 452 2. If you are including theoretical results...
- 453 (a) Did you state the full set of assumptions of all theoretical results?[Yes] Our theoretical  
454 results are of two nature: a bound in Proposition 1, and a guarantee on convergence in  
455 Proposition 2, which has no direct consequence on our empirical findings, yet remain  
456 useful. Theory is not our main contribution, but rather algorithms.
- 457 (b) Did you include complete proofs of all theoretical results?[Yes] all proofs are in the  
458 appendix. Space in the main body of the paper was prioritized to include experimental  
459 validation, which, for this non-convex problem, we believe to be equally important.
- 460 3. If you ran experiments...
- 461 (a) Did you include the code, data, and instructions needed to reproduce the main ex-  
462 perimental results (either in the supplemental material or as a URL)?[Yes] We have  
463 included portions of the code that we have used. We pledge to make the entire code  
464 available later in the reviewing process.
- 465 (b) Did you specify all the training details (e.g., data splits, hyperparameters, how they were  
466 chosen)?[Yes] The main contribution is compute efficiency, that we have considered  
467 across several parameter choices.
- 468 (c) Did you report error bars (e.g., with respect to the random seed after running ex-  
469 periments multiple times)?[N/A] Our experiments are deterministic, since we use a  
470 predefined initialization.
- 471 (d) Did you include the total amount of compute and the type of resources used (e.g., type  
472 of GPUs, internal cluster, or cloud provider)?[Yes] The experiments were run with  
473 basic computational means, a macbook pro.
- 474 4. If you are using existing assets (e.g., code, data, models) or curating/releasing new assets...
- 475 (a) If your work uses existing assets, did you cite the creators?[Yes] We have reused a  
476 single toolbox, and accessed data available publicly.
- 477 (b) Did you mention the license of the assets? [Yes] All licenses are open source, see  
478 supplementary.
- 479 (c) Did you include any new assets either in the supplemental material or as a URL? [Yes]  
480 Yes, code is shared in the supplementary.
- 481 (d) Did you discuss whether and how consent was obtained from people whose data you’re  
482 using/curating? [Yes]
- 483 (e) Did you discuss whether the data you are using/curating contains personally identifiable  
484 information or offensive content? [N/A]
- 485 5. If you used crowdsourcing or conducted research with human subjects...
- 486 (a) Did you include the full text of instructions given to participants and screenshots, if  
487 applicable? [N/A]
- 488 (b) Did you describe any potential participant risks, with links to Institutional Review  
489 Board (IRB) approvals, if applicable? [N/A]

490  
491

(c) Did you include the estimated hourly wage paid to participants and the total amount spent on participant compensation? [N/A]